EDGEWOOD CHEMICAL BIOLOGICAL CENTER

U.S. ARMY RESEARCH, DEVELOPMENT AND ENGINEERING COMMAND
Aberdeen Proving Ground, MD 21010-5424

ECBC-TR-1250

IN SILICO DOCKING OF SMALL-MOLECULE INHIBITORS TO THE *ESCHERICHIA COLI* TYPE III SECRETION SYSTEM EscN ATPase

Terry J. Henderson

RESEARCH AND TECHNOLOGY DIRECTORATE

Daniel O. Carmany

BATTELLE MEMORIAL INSTITUTE
Aberdeen, MD 21001-1228

July 2014

Approved for public release; distribution is unlimited.

U.S. ARMY
RDECOM

Disclaimer

The findings in this report are not to be construed as an official Department of the Army position unless so designated by other authorizing documents.

REPORT DOCUMENTATION PAGE

Form Approved
OMB No. 0704-0188

Public reporting burden for this collection of information is estimated to average 1 hour per response, including the time for reviewing instructions, searching existing data sources, gathering and maintaining the data needed, and completing and reviewing this collection of information. Send comments regarding this burden estimate or any other aspect of this collection of information, including suggestions for reducing this burden to Department of Defense, Washington Headquarters Services, Directorate for Information Operations and Reports (0704-0188), 1215 Jefferson Davis Highway, Suite 1204, Arlington, VA 22202-4302. Respondents should be aware that notwithstanding any other provision of law, no person shall be subject to any penalty for failing to comply with a collection of information if it does not display a currently valid OMB control number. **PLEASE DO NOT RETURN YOUR FORM TO THE ABOVE ADDRESS.**

1. REPORT DATE *(DD-MM-YYYY)* 14-07-2014	**2. REPORT TYPE** Final	**3. DATES COVERED** *(From - To)* Jan 2012 – May 2013

4. TITLE AND SUBTITLE In Silico Docking of Small-Molecule Inhibitors to the *Escherichia coli* Type III Secretion System EscN ATPase	**5a. CONTRACT NUMBER**
	5b. GRANT NUMBER
	5c. PROGRAM ELEMENT NUMBER
6. AUTHOR(S) Henderson, Terry J. (ECBC); and Carmany, Daniel O. (Battelle)	**5d. PROJECT NUMBER** CBM.THERB.02.11.ECB.023
	5e. TASK NUMBER
	5f. WORK UNIT NUMBER
7. PERFORMING ORGANIZATION NAME(S) AND ADDRESS(ES) Director, ECBC, ATTN: RDCB-DRB-C, APG, MD 21010-5424 Battelle Memorial Institute, 1204 Technology Drive, Aberdeen, MD 21001-1228	**8. PERFORMING ORGANIZATION REPORT NUMBER** ECBC-TR-1250
9. SPONSORING / MONITORING AGENCY NAME(S) AND ADDRESS(ES) Defense Threat Reduction Agency, 8275 John J. Kingman Road, Stop 6201, Ft. Belvoir, VA 22060-6201	**10. SPONSOR/MONITOR'S ACRONYM(S)** DTRA
	11. SPONSOR/MONITOR'S REPORT NUMBER(S)

12. DISTRIBUTION / AVAILABILITY STATEMENT
Approved for public release; distribution is unlimited.

13. SUPPLEMENTARY NOTES

14. ABSTRACT

The type III secretion system (T3SS) is a supermolecular construct that allows many Gram-negative pathogens to translocate effector virulence proteins directly into host cells in a process requiring adenosine triphosphate (ATP) hydrolysis. We used in silico molecular modeling and computational chemistry to determine the conformations of three different small-molecule compounds when bound to EscN, the T3SS ATPase of enteropathogenic *Escherichia coli*. Each compound was shown to separately bind EscN within or very close to its active site and to effectively inhibit catalytic activity. Two structurally related compounds were observed to adopt extended conformations in the active-site cleft and essentially occupied the entire cleft, which obstructed the ATP binding including the formation of ATP-EscN non-covalent interactions and hydrogen bonds. Both compounds appeared to span the region in the active site with Phe355 and Gln426, residues that are essential for forming π-stacking interactions and hydrogen bonds with the adenosine base of the ATP substrate. In contrast, the third compound appeared to fold upon itself in the EscN active-site cleft to adopt a very compact conformation that occupied only one side of the cleft. Our goal was to determine the three-dimensional structures of the compound–EscN complexes for designing lead compounds and ultimately develop broad-spectrum therapeutics against T3SS pathogens.

15. SUBJECT TERMS

Adenosine triphosphatase (ATPase)	Broad-spectrum antibiotic	Drug discovery
Enzyme inhibitors	Enzyme structure	Injectosome
Molecular modeling	Protein docking	Type III secretion system

16. SECURITY CLASSIFICATION OF:			**17. LIMITATION OF ABSTRACT**	**18. NUMBER OF PAGES**	**19a. NAME OF RESPONSIBLE PERSON** Renu B. Rastogi
a. REPORT U	**b. ABSTRACT** U	**c. THIS PAGE** U	UU	28	**19b. TELEPHONE NUMBER** *(include area code)* (410) 436-7545

Blank

PREFACE

The work described in this report was authorized under Defense Threat Reduction Agency (DTRA; Ft. Belvoir, VA) project no. CBM.THERB.02.11.ECB.023.

The work was started in January 2012 and completed in May 2013.

The use of either trade or manufacturers' names in this report does not constitute an official endorsement of any commercial products. This report may not be cited for purposes of advertisement.

This report has been approved for public release.

Acknowledgments

The authors would like to acknowledge DTRA for funding this research.

Blank

CONTENTS

1. INTRODUCTION 1

2. EXPERIMENTAL PROCEDURES 2

2.1 Small-Molecule YscN Inhibitors 2
2.2 Bacterial Agents and Preparation 3
2.3 Macrophage Preparation 3
2.4 Infection Assay 3
2.5 In Silico Docking of Small Molecules to the EscN ATP Site 4

3. RESULTS AND DISCUSSION 5

3.1 Inhibition Activity and Mechanism 5
3.2 Broad-Spectrum Antibiotic Potential 6
3.3 Structures of Inhibitor–EscN Complexes 7

4. CONCLUSIONS 12

LITERATURE CITED 15

ACRONYMS AND ABBREVIATIONS 17

FIGURES

1. Schematic of T3SS....1

2. Chemical structures for compounds 2834, 3624, and 9652....3

3. Compounds 2834, 3624, and 9652 inhibit the replication of four human pathogen species in murine macrophages....6

4. In silico modeling results illustrate the EscN protein structure and its complexes with the small-molecule inhibitors....8

5. Compounds 2834 and 3624 occupy much of the same space in the EscN active-site cleft, but compound 9652 occupies different space....10

6. In silico modeling reveals all EscN amino acids in close proximity to compounds 2834, 3624, and 9652 when bound to the ATPase....11

TABLE

1. Closest Intermolecular Distances between EscN and Compounds 2834, 3624, and 9652, Derived from in Silico Inhibitor–EscN Complexes....10

IN SILICO DOCKING OF SMALL-MOLECULE INHIBITORS TO THE *ESCHERICHIA COLI* TYPE III SECRETION SYSTEM EscN ATPase

1. INTRODUCTION

Using the type III secretion system (T3SS, see Figure 1) allows many Gram-negative pathogens to translocate effector virulence proteins directly into host cells, which permits pathogen survival and replication and evades the host immune response at the same time. These pathogens are complex, multiprotein assemblies that require the involvement of pathogen cytoplasmic chaperone proteins and adenosine triphosphate (ATP) hydrolysis. ATP hydrolysis is believed to provide the energy for decoupling virulence factors from the chaperones. Furthermore, this decoupling is believed to begin the movement of the unfolded chaperone proteins through the highly charged interior of the T3SS needle and into the host cell, where it ultimately folds into its native structure. Pathogens with deleted T3SS ATPase genes have been observed to lose all virulence in animal models. ATPases that were tested include EscN (enteropathogenic *Escherichia coli*), InvC (*Salmonella*), Spa47 (*Shigella flexneri*), BsaS and SpaL (*Burkholderia mallei* and *Burkholderia pseudomallei*, respectively), and YscN (*Yersinia pestis*).

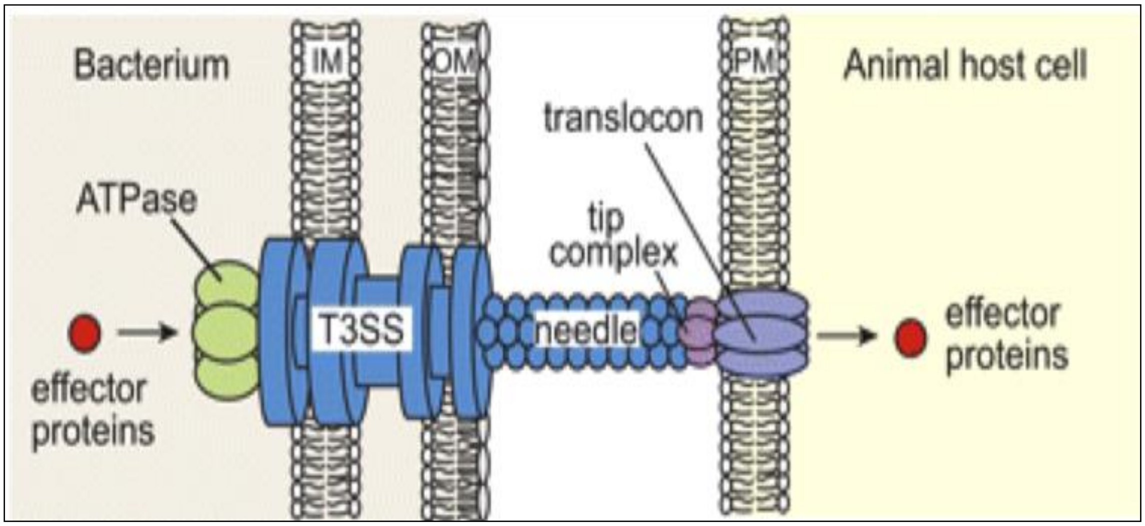

Figure 1. Schematic of T3SS. During infection, the needle is anchored into the pathogen's inner (IM) and outer (OM) membranes and extends into the host's plasma membrane (PM). Six ATPases at the needle's base are believed to remove the effector proteins from their chaperones, allowing effector delivery through the needle directly into the host (from Büttner and He, 2009).

Previously, Swietnicki and co-workers (2011) reported a panel of 50 small molecules that bind the YscN ATP site, and separately demonstrated their abilities to inhibit YscN activity and protect eukaryotic cells from *Y. pestis* infection. We tested all members of the panel for broad-spectrum activity by measuring their ability to confer macrophage survivability against infection by human pathogens. We identified three molecules that had broad-spectrum potential. To better understand the binding of each of the three compounds to T3SS ATPases, in the hope of developing more promising therapeutics, we conducted an in silico structural investigation of the three inhibitor–EscN complexes because EscN was the only T3SS ATPase crystal structure reported to date (Zarivach et al., 2007). The two inhibitors demonstrating the most-promising broad-spectrum activity against four human pathogenic species displayed similar inhibition patterns, as a function of concentration. Our in silico investigation revealed that two inhibitors in the EscN ATP site had similar orientations, where each adopted an extended conformation that spanned essentially the entire site and completely blocked ATP access. In silico data for the third YscN inhibitor revealed a compact, highly folded conformation that occupied only one side of the ATP site, leaving the other side somewhat accessible to the ATP substrate. Our in silico results are reported herein, along with our preliminary broad-spectrum testing data for the three YscN inhibitors.

2. EXPERIMENTAL PROCEDURES

2.1 Small-Molecule YscN Inhibitors

Swietnicki et al. (2011) described the in silico screening of the ZINC[*] chemical database (Irwin and Shoichet, 2005), which consisted of ~5×10^6 commercially available compounds, to identify a panel of small-molecule YscN inhibitors. Chosen to test their potential for broad-spectrum activity, three compounds in the panel were assigned in-house numbers of 2834 (ZINC 11326727), 3624 (ZINC 11452647), and 9652 (ZINC 10955611), as shown in Figure 2. The compounds were purchased as dry powders from either Life Chemicals, Inc. (Burlington, Canada) or Enamine Ltd. (Kiev, Ukraine). Stock solutions of the compounds in dimethylsulfoxide (DMSO) and/or dimethylformamide (DMF) were made in-house (U.S. Army Edgewood Chemical Biological Center; Aberdeen Proving Ground, MD). Stock solutions were stored at –20 °C in amber glass vials. The thawed stock solutions were serially diluted with DMSO when required and then stored at –20 °C in amber glass vials as well.

---

[*] ZINC is a recursive acronym for “zinc is not commercial”.

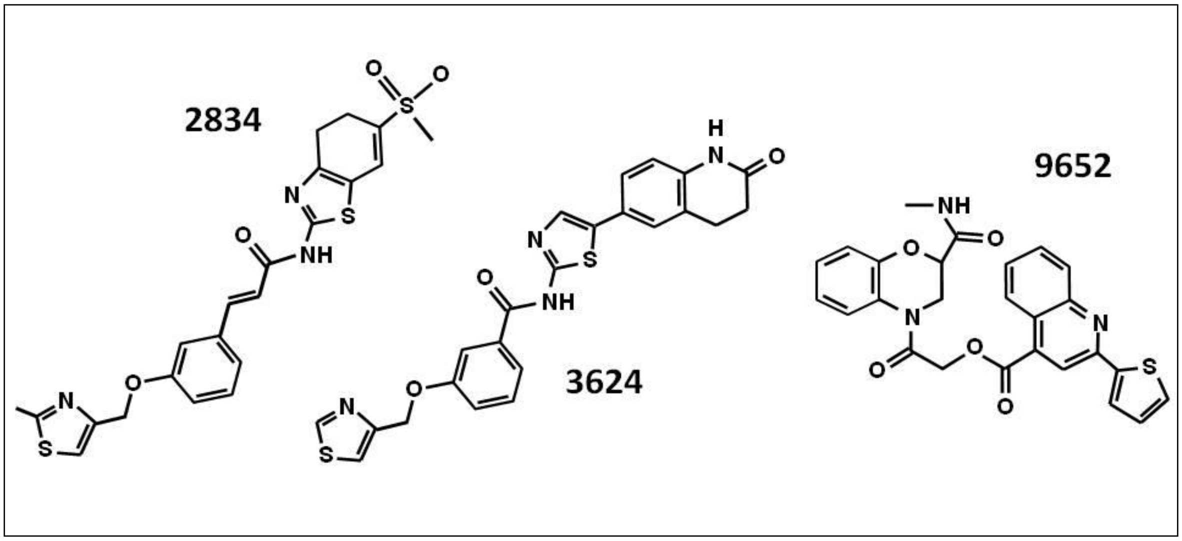

Figure 2. Chemical structures for compounds 2834, 3624, and 9652.

2.2 Bacterial Agents and Preparation

Stocks of *E. coli* strain RDEC-1, *Salmonella* serotype Enteritidis, *B. pseudomallei* strain 1026B, and *S. flexneri* were separately used to inoculate 3 mL broth cultures. After overnight incubation at 30 °C, the cultures were diluted 1:100 (v:v) in warm Dulbecco's modified Eagle's medium (DMEM; Life Technologies; Grand Island, NY) containing 10% fetal bovine serum (FBS; Life Technologies) that was supplemented with various concentrations of a single inhibitor compound.

2.3 Macrophage Preparation

RAW 264.7 murine macrophages (Sigma-Aldrich; St. Louis, MO) were maintained in DMEM containing 10% FBS and antibiotics. One day before infection, the cells were harvested and seeded into a 96-well plate at 1.2×10^5 cells/well in DMEM supplemented with 10% FBS, without antibiotics. The macrophages were then incubated overnight at 37 °C with 5.0% gaseous carbon dioxide.

2.4 Infection Assay

All media were removed from the plates by aspiration, and warm bacterial inhibitor solution was added to each well. After the well plates were incubated for 2 h at 37 °C with a 5.0% gaseous carbon dioxide atmosphere, the bacterial/inhibitor solution was removed, and all wells were washed with warm phosphate-buffered saline (PBS). The macrophages were then placed in DMEM that was supplemented with 10% FBS, kanomycin (to kill extracellular bacteria), and one of the three specific inhibitor compounds. The macrophages were then incubated for 3 h at 37 °C with 5.0% gaseous carbon dioxide. After all media was aspirated from the wells, the cells were washed again with warm PBS. Ice-cold 0.25% Triton X-100 (Thermo Fisher Scientific; Waltham, MA) solution was added to the wells to facilitate the release of macrophages from the well walls. Then the resulting suspensions were vigorously mixed to disrupt the macrophages and release the intracellular bacteria. Finally, samples were serially diluted and plated onto growth media. Cells were counted using a Spiral Biotech Qcounter (Advanced Instruments; Norwood, MA).

2.5 In Silico Docking of Small Molecules to the EscN ATP Site

Atomic coordinates for the compounds 2834, 3624, and 9652 were downloaded directly from the ZINC chemical database (Irwin and Shoichet, 2005) website (http://zinc.docking.org/) in *mol2* file format. The files were converted to the *pdbqt* format with the Autodock Tools 1.5.4 software program (Molecular Graphics Laboratory, The Scripps Research Institute; La Jolla, CA).

The X-ray crystal coordinates of the EscN protein (Zarivach et al., 2007) were downloaded in *pdb* file format from the Research Collaboratory for Structural Biology Protein Data Bank (http://www.rcsb.org, deposition number 2OBL). The Chimera 1.6.2 software program (University of California; San Francisco, CA) was used to remove all coordinates for water and counterion (Ca^{2+}, acetate, and imidazole) atoms and to add coordinates for all EscN protons (Petterson et al., 2004). The Chimera program was also used with the AMBER force field (Ponder and Case, 2003) to conduct 500 iterations of the steepest-descent energy minimization on the EscN protein to relieve any highly unfavorable atomic clashes derived from the added protons. This was followed by 500 iterations of conjugate gradient minimization to converge on the local, lowest-energy conformation. Visual inspection of the protein conformation before and after energy minimization revealed only occasional, small differences from the original coordinates of the carbon, nitrogen, oxygen, and sulfur atoms, with >>1 Å difference in any one dimension.

Coordinates for the final EscN conformation were archived to computer disk in *pdbqt* file format using the Autodock Tools program. Docking of the inhibitor compounds to the EscN ATP site was achieved using the Autodock Vina 1.1.2 program (Trott and Olson, 2010) with the inhibitor compound and EscN *pbqt* files. EscN was modeled as a conformationally rigid protein; however, the small-molecule inhibitors were allowed complete rotation about all torsion angles. The energy grid center was defined as the geometrical center of the ATP-binding site ($x = 14.177$ Å, $y = 11.761$ Å, and $z = –3.754$ Å) with a total volume of $28 \times 26 \times 24$ Å^3. For each ligand, a thorough search of its conformational space (exhaustiveness of 100) was conducted to identify its nine conformational poses with the highest binding affinities for the ATP site, as defined by the default scoring function. In all cases, conformational poses had root mean square deviations (RMSDs) between 1.5 and 14.0 Å, relative to that with the highest binding affinity. For each of these poses, a final energy minimization of the inhibitor–EscN complexes were conducted by again modeling EscN as a conformationally rigid protein and allowing complete rotation about all YscN-inhibitor torsion angles. The Chimera program, with the AMBER force field, was used to conduct 500 iterations of steepest-descent energy minimization followed by 20,000 iterations of conjugate gradient minimization. The progress of each complex energy minimization was visualized using the Chimera program to ensure they converged on a single conformational pose. All software programs were installed and run on an iMac computer using the Mac OS X v10.6.3 operating system (Apple Computer; Cupertino, CA).

3. RESULTS AND DISCUSSION

3.1 Inhibition Activity and Mechanism

The results obtained from investigating the abilities of compounds 2834, 3624, and 9652 to inhibit infection in murine macrophages against *B. pseudomallei* strain 1026B, *E. coli* strain RDEC-1, *Salmonella* serotype Enteritidis, and *S. flexneri* are summarized in Figure 3. Observation of the results revealed that all three compounds were capable of inhibiting the replication of each of the four human pathogens, with ≥60% inhibition activity at 10 µM concentrations. Titrations performed to determine the compounds' activity ranges revealed that compound 3624 displayed the highest combined activity against the four pathogens, with ~70% specific inhibition against *B. pseudomallei* strain 1026B at 900 nM. Figure 3 also shows that the somewhat structurally similar compounds, 2834 and 3624, displayed similar inhibition profiles. For example, at 10 µM, both compounds were used to completely inhibit *E. coli* RDEC-1 and *S. flexneri*. At the same concentrations, these compounds almost completely inhibited *Salmonella* serotype Enteritidis infection. Inhibition of the *B. pseudomallei* strain 1026B infection was observed to be the most difficult to accomplish using these compounds; both displayed results of ~70% inhibition at 10 µM. Against all four pathogens, inhibition using compound 9652 was significantly less efficient than when either of the other two compounds was used. This finding revealed a very different inhibition profile for compound 9652 in comparison with compounds 2834 and 3624. It was reasonable to assume that the three compounds were able to bind T3SS ATPase sites, or very close to these sites, and inhibit pathogenic virulence for the following reasons: (1) Test compounds were originally selected using in silico methods for binding the YscN ATPase site; (2) two compounds, 2834 and 9652 (compound 3624 was not tested), were shown to directly inhibit YscN activity (Swietnicki et al., 2011); and (3) T3SS ATPase structure was highly conserved among the pathogens.

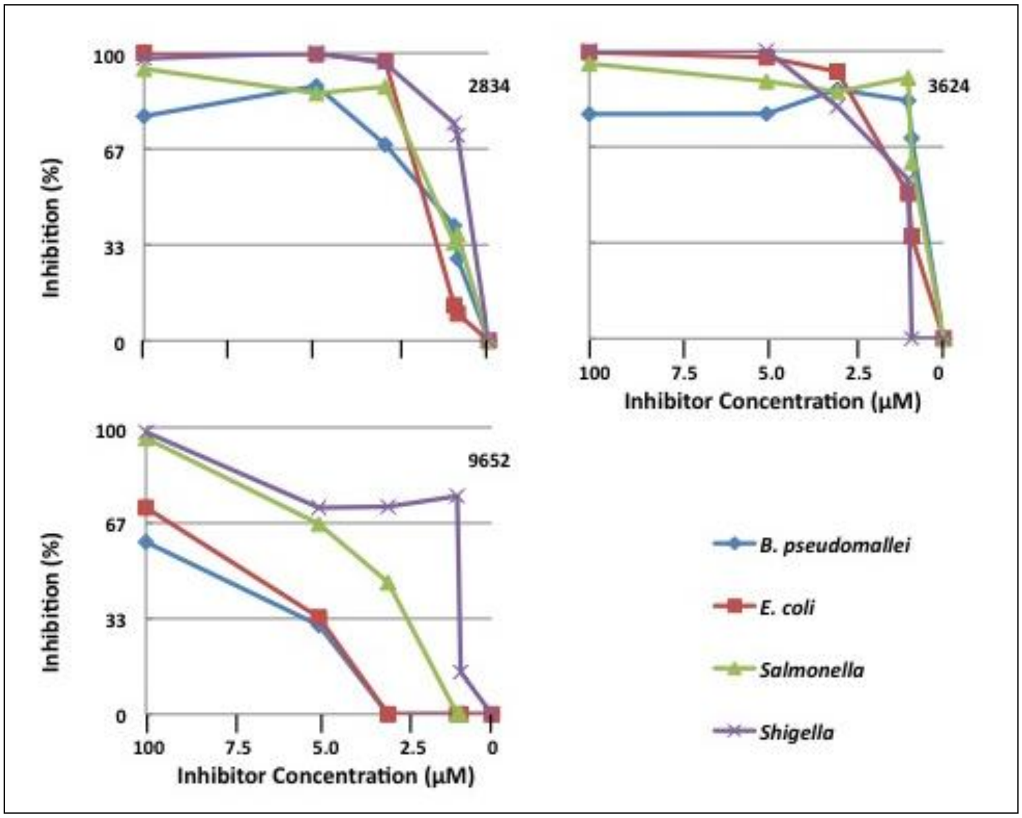

Figure 3. Compounds 2834, 3624, and 9652 inhibit the replication of four human pathogen species in murine macrophages.

3.2 Broad-Spectrum Antibiotic Potential

Our preliminary results revealed that the three compounds could inhibit T3SS virulence in five bacterial species (including *Bulkholderia thailandensis*, not shown in Figure 3). Therefore, these compounds have potential for use as broad-spectrum therapeutics. Although they did inhibit T3SS-specific virulence, the compounds were not toxic to the pathogens; their eradication came about as a consequence of the host's immune system when the compounds were used as therapeutics. We have also demonstrated that the compounds were not toxic to macrophages or to Henrietta Lacks (HeLa) cells (not shown). As an added benefit for the therapeutic use of the compounds, the T3SS ATPases shared only ~25% amino acid sequence homology with human ATPases. It was, therefore, unlikely that the therapeutic use of these three compounds would inhibit the activities of human ATPases. Finally, the three compounds all complied with Lipinski's rule of five (Lipinski et al., 2001; Leeson, 2012), which are the most common guidelines used to ensure small-molecule drug solubility and permeability.

3.3 Structures of Inhibitor–EscN Complexes

To better understand the binding of compounds 2834, 3624, and 9652 to T3SS ATPase active sites for the development of more-promising therapeutic candidates, we have used in silico methods to estimate the structures of three inhibitor–EscN complexes. The ATP-binding site (rendered as a solvent-accessible surface model in Figure 4A) has already been described in detail when bound to one adenosine diphosphate (ADP) molecule, as shown in Figure 4B. The ATP-binding site is located primarily in the central Rossmann-fold domain of the ATPase (Walker et al., 1982). ADP has ~50% of its surface (~173 Å^2) buried in the active-site cleft, where it forms several favorable, non-covalent interactions. The binding site for the substrate phosphate groups is composed of residues 179–185, forming the conserved phosphate-binding loop (P-loop) of the ATPase (Abrahams et al., 1994; Groth, 2002; Shirakihara et al., 1997). These residues, sometimes referred to as the Walker motif, are colored red in Figure 4. The adenosine base is bound by π-stacking to the aromatic side chain of Phe355[†], as well as by direct hydrogen bonding from N6[‡] to the carbonyl oxygen atom of Gln426[§] and by a water-bridged hydrogen bond from the base of N7[**] to the carbonyl oxygen atom of the conserved Gly182[††] in the P-loop. In Figure 4, the amino acid residues, Phe355 and Gln426, are colored blue and cyan, respectively.

Figure 4B shows the in silico docking results for the three small-molecule inhibitors with the EscN active site and the crystal coordinates of ADP bound to the same site for comparison. The orientation of the EscN protein in each of the three views, as well as that of ADP, differs slightly from one image to the next so that the inhibitor conformation can be viewed unobstructed in the active-site cleft. Observation of the figure reveals that the structurally related compounds 2834 and 3624 occupy the active-site cleft in a similar manner. Both compounds are shown in an extended conformation, where all but their terminal thiazole rings and part of the directly attached ethoxy groups lie approximately in a single plane. Additionally, both inhibitors occupy essentially the entire active-site cleft, including the P-loop and the region containing Phe355 and Gln426, which are important for forming π-stacking interactions and hydrogen bonds, respectively, with the adenosine base of the substrate. These inhibitor conformations and their orientations within the active-site cleft not only sterically hinder the ATP substrate from occupying the active-site cleft; they also obstruct the formation of non-covalent interactions and hydrogen bonding between the substrate and the EscN protein. The similarities may be responsible for the similar inhibition profiles that were observed for compounds 2834 and 3624 (Figure 3).

[†] Phe355: phenylalanine residue at amino acid position 355

[‡] N6: nitrogen atom site six

[§] Gln426: glutamine residue at amino acid position 426

[**] N7: nitrogen atom site seven

[††] Gly182: glycine residue at amino acid position 182

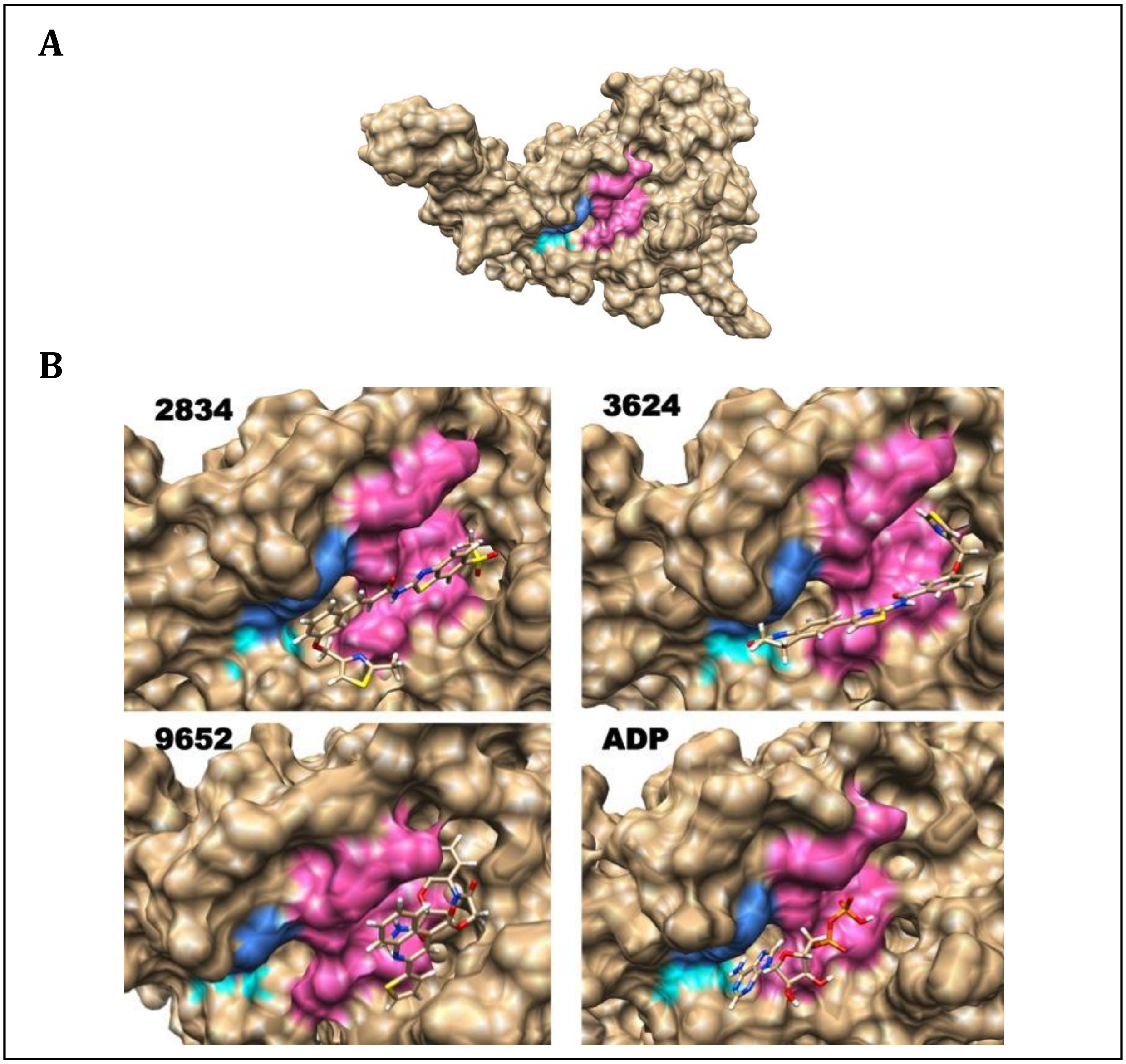

Figure 4. In silico modeling results illustrate the EscN protein structure and its complexes with the small-molecule inhibitors. (A) Solvent-accessible area of EscN rendered from its crystal coordinates at 1.8 Å resolution (Zarivach et al., 2007). The ATP-binding cleft appears in the center of the model in color. (B) Compounds 2834, 3624, and 9652 and ADP (Zarivach et al., 2007) bound in the EscN ATP-binding site. Residues 179–185 are colored red, and residues 355 and 426 are colored blue and cyan, respectively.
(See text for an explanation of residue colors.)

Upon further examination of Figure 4, the compounds are observed to be oriented ~180° relative to one another when bound in the active-site cleft. For example, when compound 2834 is bound in the active site, the terminal thiazole ring appears on the side of the active-site cleft containing Gln426 (cyan). However, the analogous ring of compound 3624 appears at the other end of the active-site cleft, almost completely surrounded by residue side chains of the P-loop. On the other hand, the binding of compound 9652 to the EscN active-site cleft appears to be a distinct departure from the results observed for the other compounds. When bound in the EscN-active site, compound 9652 appears to fold in upon itself and adopt a compact conformation. In addition, rather than spanning the entire active-site cleft, the compact compound 9652 conformation appears on only one side of the cleft, surrounded on one side by the residue side chains of the P-loop. Although it does block substrate access to the P-loop, the compact conformation and orientation of the compound in the active-site cleft leaves the side chains of Phe355 and Gln426 completely open to access from the substrate's adenosine base. This active-site orientation could account for the somewhat lower inhibition activity of compound 9652 relative to the others (Figure 3).

The in silico derived coordinates for each of the three inhibitors bound to the EscN active site have been superimposed upon one another to create Figure 5. This figure shows the three-dimensional space occupied by each conformational pose within the active-site cleft. The crystal coordinates for ADP bound to the active site are also included for direct comparison. Figure 5 clearly shows the very different space occupied by the compound 9652 conformation (cyan), relative to those of the other two compounds and that of ADP. The compound 9652 conformation shares a small amount of space with the ADP conformation (tan, blue, white, red, and orange), where its terminal phosphate group slightly overlaps with the methyl protons of the compound's methylcarbamoyl group.

Although the terminal phosphate group of the ATP substrate would undoubtedly be hindered by the inhibitor conformation, most of the substrate, including its adenosine base, is completely unobstructed to the EscN active site by the compound 9652 conformation. Figure 5 shows the similarities described in the previous paragraphs for the bound conformations of compounds 2834 (green) and 3624 (violet) and their occupation of much of the same space within the EscN active site. Specifically, their extended conformations appear to almost parallel each other in three-dimensional space, and they overlap at six different points (not shown in the figure). The conformations of compounds 2834 and 3624 share most of the same space as the ADP-bound conformation, and only the ADP adenosine ring amino group is unobstructed by the inhibitor conformations. These similarities, again, are consistent with the similar inhibition profiles observed for compounds 2834 and 3624 (Figure 3).

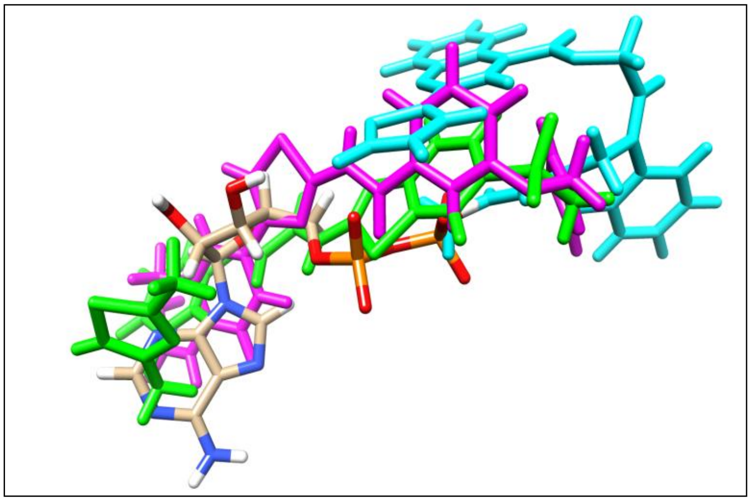

Figure 5. Compounds 2834 (green) and 3624 (violet) occupy much of the same space in the EscN active-site cleft, but compound 9652 (cyan) occupies different space. The crystal coordinates for ADP bound to the active-site cleft (Zarivach et al., 2007) are colored tan, blue, white, red, and orange; atoms and bonds and are included for comparison.
(See text for an explanation of the figure.)

Figure 6 shows EscN amino acids with ≤3.0 Å between their side-chain atoms and the side-chain atoms of the bound inhibitor conformation for each inhibitor–EscN complex. Although the figure was created to eliminate any overlap between the amino acid side chains and the inhibitors, their intermolecular distances can be difficult to observe in the figure. Therefore, the closest intermolecular distances for each of the inhibitor–EscN complexes are reported in the following table.

Table 1. Closest Intermolecular Distances between EscN and Compounds 2834, 3624, and 9652, Derived from in Silico Inhibitor–EscN Complexes

EscN	Closest Atom-to-Atom Distance (Å)*		
Amino Acid	Compound 2834	Compound 3624	Compound 9652
Lys183	2.46	2.88	–
Ser184	3.00	2.63	–
Thr185	2.39	2.72	–
Arg207	–	–	2.70
Glu210	1.87	3.00	2.46
Glu213	–	–	2.49
Arg270	–	–	2.11
Leu321	–	–	1.97
Asn353	2.99	3.00	–
Phe355	2.57	1.67	–

* All distances are ≤3.0 Å. Larger distances are not listed.

– Distances are >3.0 Å.

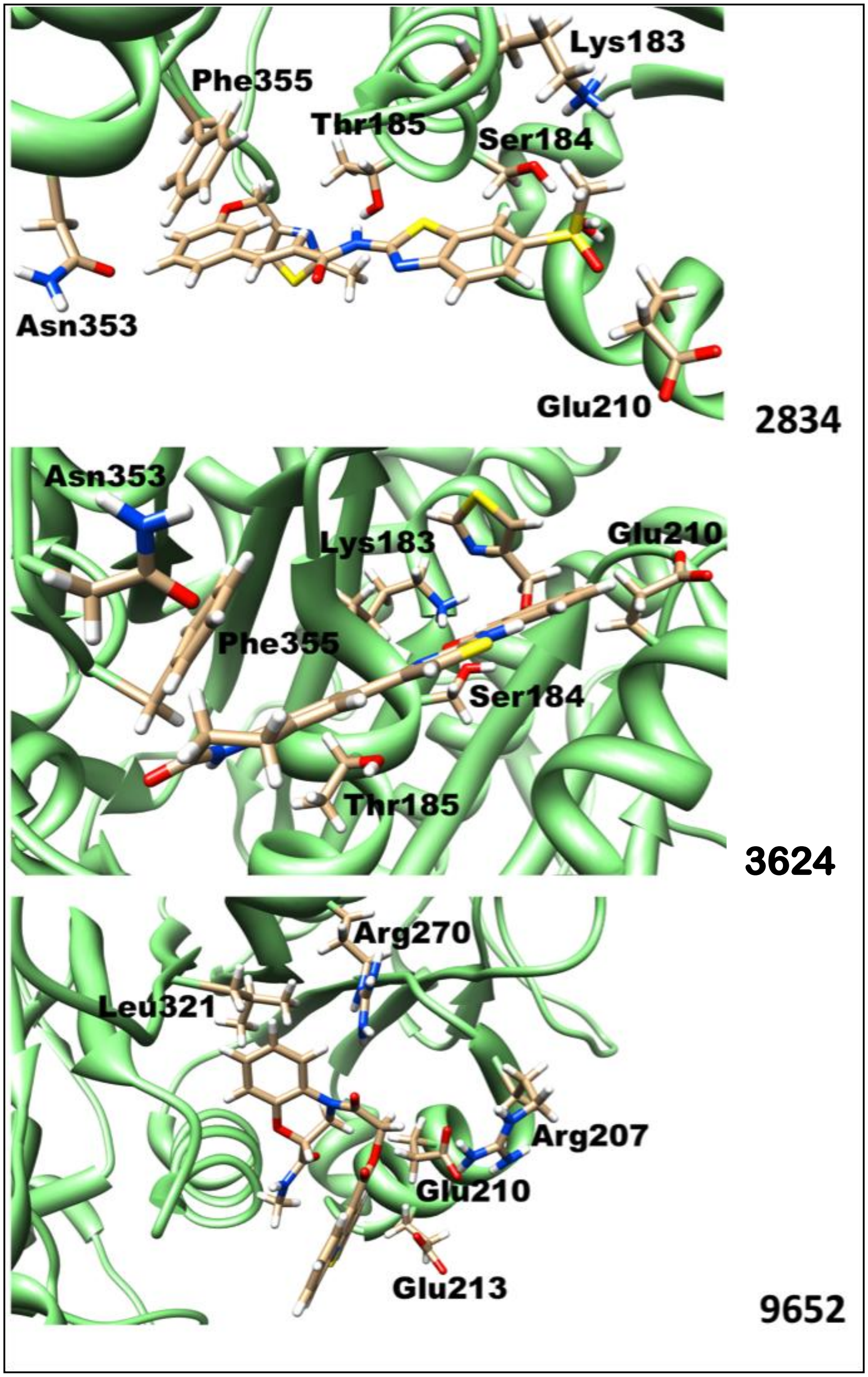
Phe355
Lys183
Thr185
Ser184
Asn353
Glu210
2834
Asn353
Lys183
Glu210
Phe355
Ser184
Thr185
3624
Arg270
Leu321
Arg207
Glu210
Glu213
9652

Figure 6. In silico modeling reveals all EscN amino acids in close proximity to compounds 2834, 3624, and 9652 when bound to the ATPase. All amino acid side chains shown have atom-to-atom distances of ≤3.0 Å between the side chain and the compound.

4. CONCLUSIONS

In silico molecular modeling and computational chemistry was used to determine the conformations of three different small-molecule compounds (compounds 2834, 3624, and 9652) when bound to the active site of EscN. In each case, the compounds were shown to bind the EscN protein within or in close proximity to its active site (Figure 3). Our goal was to determine the three-dimensional structures of the respective compound–EscN complexes to initiate the design of compounds that could be used as lead compounds in the development of high-potency, broad-spectrum therapeutics against T3SS pathogens. Although such an endeavor would benefit tremendously from the crystal structures of the compound–EscN complexes, ATPases are difficult to crystallize, and efforts to crystallize T3SS ATPases have not been successful to date. At the time of this study, EscN was the only T3SS ATPase ever reported to form X-ray-quality crystals and, therefore, its crystal structure was the only ATPase structure suitable for our use.

Of the three small-molecule inhibitors investigated, compounds 2834 and 3624 displayed the best potential for use as lead compounds in the development of broad-spectrum therapeutics. This was determined from their ability to inhibit human pathogen replication in murine macrophages. Compounds 2834 and 3624 share many structural features (Figure 2) and display similar inhibition profiles (Figure 3). Moreover, as revealed by our molecular modeling and computational chemistry results (Figures 4, 5, and 6), these compounds may occupy the EscN active site in a similar manner (Figure 4). In addition, both compounds occupy the active site in a manner similar to ADP in the EscN crystal lattice (Figure 5). Therefore, it is reasonable to assume that both compounds occupy the site in a manner similar to that of the ATP substrate as well. Compounds 2834 and 3624 both adopt extended conformations in the active-site cleft, occupy essentially the entire active site, and obstruct ATP substrate binding. The two compounds also form non-covalent interactions and hydrogen bonding between the ATP substrate and EscN protein. Both compounds appear to occupy the region of the active site that contains Phe355 and Gln426, which are residues that are essential for forming π-stacking interactions and hydrogen bonds with the adenosine base of the ATP substrate. It is interesting to note that our in silico results did not show compound 9652 occupying this region of the active site nor any active site regions close to it. This finding was consistent with the results shown in Figure 3, with compound 9652 exhibiting significantly lower inhibition activities for human pathogens in murine macrophages relative to those of the other two compounds.

There are certain caveats to consider when deriving new lead compounds from preliminary in silico data such as ours. For example, the docking of our small-molecule compounds to the EscN active site was conducted with rigid EscN models and did not allow conformational flexibility in the protein’s active site. Although most in silico docking protocols rely on this approach, there was much speculation that protein conformational flexibility is an integral part of the ligand and substrate recognition and binding processes. However, direct evidence of such contributions from protein conformational flexibility remains largely elusive to date (Estrada et al., 2014). Additionally, our docking procedure excluded explicit solvent water molecules, which is another common practice for docking protocols. Although such simplifications are typically employed to decrease in silico computation times, their use can potentially lead to a compromised representation of the EscN protein in solution. Therefore, we cannot rule out the possibility that the actual conformations of our small-molecule compounds bound to the EscN active site are significantly different from those detailed herein. Our results, therefore, should be validated with at least some experimental data from authentic EscN complexes with our small-molecule inhibitors before developing lead compounds from them.

The most direct techniques to validate our EscN-inhibitor structures would be to collect X-ray diffraction data from EscN–inhibitor complex crystals or biomolecular nuclear magnetic resonance (NMR) data of appropriately prepared complexes. Because ATPase crystallization is inherently problematic (Zarivach et al., 2007), it is likely that the NMR approach would be the best path forward. Preliminary data could be collected on each EscN–inhibitor complex to identify all protons of the inhibitor molecule within close proximity (>5 Å) of the EscN protons by using saturation transfer difference (STD) NMR spectroscopy (Silvestre et al., 2013; Mayer and Meyer, 1999). The technique could be performed easily without labeling the EscN protein with ^{2}H, ^{13}C, or ^{15}N isotopes or without assigning EscN NMR signals to individual protons. Together with the EscN crystal structure, these data can be used to validate our proposed complex structures or to generate new complex structures that are consistent with the STD data. Such investigations alone may yield enough information to begin developing lead compounds. Later NMR efforts could concentrate on using nuclear Overhauser effect spectroscopy, usually referred to as NOESY, to determine the solution structures of the EscN–inhibitor complexes or those of the inhibitors with T3SS ATPases from other bacterial species. With ~350 amino acid residues (~38 kDa), a T3SS ATPase monomer, bound to one of our inhibitors, would be small enough for NMR structural determinations using high-field spectrometers (>16.45 tesla). More importantly, it is likely that the structures of the complexes would need to be solved to successfully develop lead compounds.

Blank

LITERATURE CITED

Abrahams, J.P.; Leslie, A.G.; Lutter, R.; Walker, J.E. Structure at 2.8 Å Resolution of the F1-ATPase from Bovine Heart Mitochondria. *Nature* **1994**, *370*, 621–628.

Büttner, D.; He, S.Y. Type III Protein Secretion in Plant Pathogenic Bacteria. *Plant Physiol.* **2009**, *150*, 1656–1664.

Estrada, D.F.; Skinner, A.L.; Laurence, J.S.; Scott, E.E. Human Cytochrome P450 17A1 Conformational Selection: Modulation by Ligand and Cytochrome b5. *J. Biol. Chem.* **2014** [Intranet publication ahead of print].

Groth, G. Structure of Spinach Chloroplast F1-ATPase Complexed with the Phytopathogenic Inhibitor Tentoxin. *Proc. Natl. Acad. Sci. USA* **2002**, *99*, 3464–3468.

Irwin, J.J.; Shoichet, B.K. ZINC-A Free Database of Commercially Available Compounds for Virtual Screening. *J. Chem. Inf. Model* **2005**, *45*, 177–182.

Leeson, P. Drug Discovery: Chemical Beauty Contest. *Nature* **2012**, *481*, 455–456.

Lipinski, C.A.; Lombardo, F.; Dominy, B.W.; Feeney, P.J. Experimental and Computational Approaches to Estimate Solubility and Permeability in Drug Discovery and Drug Development Settings. *Adv. Drug Del. Rev.* **2001**, *46*, 3–26.

Mayer, M.; Meyer, B. Characterization of Ligand Binding by Saturation Transfer Difference NMR Spectroscopy. *Angew. Chem. Int. Ed.* **1999**, *38*, 1784–1788.

Pettersen, E.F.; Goddard, T.D.; Huang, C.C.; Couch, G.S.; Greenblatt, D.M.; Meng, E.C.; Ferrin, T.E. USCF Chimera: A Visualization System for Exploratory Research and Analysis. *J. Comput. Chem.* **2004,** *25*, 1605–1612.

Ponder, J.W.; Case, D.A. Force Fields for Protein Simulations. *Adv. Prot. Chem.* **2003**, *66*, 27–85.

Shirakihara, Y.; Leslie, A.G.; Abrahams, J.P.; Walker, J.E.; Ueda, T.; Sekimoto, Y.; Kambara, M.; Saika, K.; Kagawa, Y.; Yoshida, M. The Crystal Structure of the Nucleotide-Free Alpha 3 Beta 3 Subcomplex of F1-ATPase from the Thermophilic *Bacillus* PS3 is a Symmetric Trimer. *Structure* **1997**, *15*, 825–836.

Silvestre, H.L.; Blundell, T.L; Abell, C.; Ciulli, A. Integrated Biophysical Approach to Fragment Screening and Validation for Fragment-Based Lead Discovery. *Proc. Natl. Acad. Sci. USA* **2013**, *110*, 12984–12989.

Swietnicki, W.; Carmany, D.; Retford, M.; Guelta, M.; Dorsey, R.; Bozue, J.; Lee, M.S.; Olson, M.A. Identification of Small-Molecule Inhibitors of *Yersinia pestis* Type III Secretion System YscN ATPase. *PLoS ONE*. **2011**, *6*(5), e19716, DOI: 10.1371/journal.pone.0019716.

Trott. O.; Olson, A.J. Autodock Vina: Improving the Speed and Accuracy of Docking with a New Scoring Function, Efficient Optimization and Multithreading. *J. Comput. Chem.* **2010**, *31*, 455–461.

Walker, J.E.; Saraste, M.; Runswick, M.J.; Gay, N.J. Distantly Related Sequences in the Alpha- and Beta-Subunits of ATP Synthase, Myosin, Kinases and other ATP-Requiring Enzymes and a Common Nucleotide Binding Fold. *EMBO J.* **1982**, *1*, 945–951.

Zarivach, R.; Vuckovic, M.; Deng, W.; Finlay, B.B.; Strynadka, C.J. Structural Analysis of a Prototypical ATPase from the Type III Secretion System. *Nat. Struct. Mol. Biol.* **2007**, *14*, 131–137.

ACRONYMS AND ABBREVIATIONS

ADP	adenosine diphosphate
ATP	adenosine triphosphate
ATPase	adenosine triphosphatase enzyme
B. pseudomallei	*Bulkholderia pseudomallei* (bacterial species)
B. thailandensis	*Bulkholderia thailandensis* (bacterial species)
DMEM	Dulbecco's modified Eagle's medium
DMF	dimethylformamide
DMSO	dimethylsulfoxide
E. coli	*Escherichia coli* (bacterial species)
EscN	adenosine triphosphatase of enteropathogenic *Escherichia coli* type III secretion system
FBS	fetal bovine serum
Gln426	glutamine residue at amino acid position 426
Gly182	glycine residue at amino acid position 182
HeLa	Henrietta Lacks (cell line)
N6	nitrogen atom site six
N7	nitrogen atom site seven
NMR	nuclear magnetic resonance
NOESY	nuclear Overhauser effect spectroscopy
P-loop	phosphate-binding loop (of a protein)
PBS	phosphate-buffered saline
Phe355	phenylalanine residue at amino acid position 355
RMSD	root mean square deviation
STD	saturation transfer difference (nuclear magnetic resonance spectroscopy technique)
S. flexneri	*Shigella flexneri* (bacterial species)
T3SS	type III secretion system
v:v	volume-to-volume ratio
Y. pestis	*Yersinia pestis* (bacterial species)
YscN	type III secretion system adenosine triphosphatase of the *Yersinia pestis* injectosome
ZINC	recursive acronym for “zinc is not commercial”

EDGEWOOD CHEMICAL BIOLOGICAL CENTER
A U.S. Army RDECOM Laboratory